

# Zero-Temperature Magnetic Transition in an Easy-Axis Kondo Lattice Model

Jian-Xin Zhu,<sup>1</sup> Stefan Kirchner,<sup>2</sup> Ralf Bulla,<sup>3</sup> and Qimiao Si<sup>2</sup>

<sup>1</sup>*Theoretical Division, Los Alamos National Laboratory, Los Alamos, New Mexico 87545, USA*

<sup>2</sup>*Department of Physics & Astronomy, Rice University, Houston, TX 77005, USA*

<sup>3</sup>*Theoretische Physik III, Elektronische Korrelationen und Magnetismus, Institut für Physik, Universität Augsburg, D-86135 Augsburg, Germany*

We address the quantum transition of a spin-1/2 antiferromagnetic Kondo lattice model with an easy-axis anisotropy using the extended dynamical mean field theory. We derive results in real frequency using the bosonic numerical renormalization group (bNRG) method and compare them with Quantum Monte Carlo results in Matsubara frequency. The bNRG results show a logarithmic divergence in the critical local spin susceptibility, signaling a destruction of Kondo screening. The  $T = 0$  transition is consistent with being second order. The bNRG results also display some subtle features; we identify their origin and suggest means for further microscopic studies.

PACS numbers: 71.10.Hf, 71.27.+a, 75.20.Hr, 71.28.+d

A sizable number of (nearly) stoichiometric heavy fermions have recently been discovered in which the antiferromagnetic transition temperature can be continuously suppressed to zero [1]. These materials have not only allowed further elucidation of the heavy fermion physics but also provided a concrete setting to address the larger question of quantum criticality. The application of the Landau paradigm considers the fluctuations of the magnetic order parameter as the primary critical modes [2]. The resulting  $T = 0$  spin-density-wave (SDW) quantum critical point (QCP) [2, 3, 4] is Gaussian. However, a host of dynamical, transport and thermodynamic data [1, 5, 6, 7, 8] suggest that the observed QCPs are non-Gaussian, indicating the existence of additional quantum critical modes. Since there is not yet a universal prescription for the identification of such emergent critical modes, microscopic considerations have been playing an important role.

One idea invokes the breakdown of the Kondo screening effect at the magnetic QCP to characterize the new critical modes [9, 10, 11]. In local quantum criticality [9], the destruction of the Kondo effect arises through the decoherence by the magnetic order parameter fluctuations. Microscopically, this picture has been studied through the extended dynamical mean field theory (EDMFT) approach [12, 13]. Here, the Kondo lattice systems are analyzed in terms of a Bose-Fermi Kondo (BFK) model, with the spectra of its fermionic and bosonic baths self-consistently determined. The EDMFT approach addresses the RKKY-Kondo competition, going beyond the seminal works of Refs. [14, 15] in ways that are important for the collapse of the Kondo scale at the magnetic QCP. It treats this competition dynamically. Equally important, it incorporates not only paramagnetic/antiferromagnetic phases with a “large” Fermi surface, but also an antiferromagnetic phase with a “small” Fermi surface (local moments not participating in the electronic Fermi volume). The critical behavior of the BFK model was shown to allow [9] a self-consistent so-

lution in which the criticality of the BFK model – with critical Kondo screening – is manifested at the magnetic QCP of the lattice. This analytical result was verified in a Quantum Monte Carlo (QMC) study of a Kondo lattice model with an easy-axis anisotropy [16]. An important question is whether the actual zero-temperature transition is second order. Earlier works at finite temperatures, using various QMC approaches, have led to some conflicting conclusions [17, 18]. The differences have been attributed to the different EDMFT equations, which handle the generated RKKY interactions on the ordered side differently [19, 20].

In this Letter, we study the magnetic transition of the anisotropic Kondo lattice model directly at zero temperature, using the recently developed bNRG method [21, 22]. Our results are important for experiments, not only because the numerical studies play an important role in the understanding of the unusual magnetic dynamics [5] (which itself was the primary initial experimental indication for the non-SDW nature of the QCP), but also because the theoretical picture has crucial predictions for other experiments that are actively being examined by on-going experiments (*e.g.*, Refs. [7, 8]). More generally, whether unconventional QCPs would be stable and relevant to realistic models/materials or tend to be preempted by first order transitions are broadly important and also arises [23] in, *e.g.*, the case of deconfined quantum criticality [24] in spin/boson lattice systems.

The Kondo lattice Hamiltonian is

$$\mathcal{H} = \sum_{ij\sigma} t_{ij} c_{i\sigma}^\dagger c_{j\sigma} + \sum_i J_K \mathbf{S}_i \cdot \mathbf{s}_{c,i} + \sum_{ij} (I_{ij}/2) S_i^z S_j^z. \quad (1)$$

Here,  $\mathbf{S}_i$  and  $\mathbf{s}_{c,i}$  represent the spins of the  $S = \frac{1}{2}$  local moment and conduction  $c$ -electrons respectively. There are 1 moment and, on average,  $x < 1$  conduction electrons, per site.  $J_K$  is the antiferromagnetic Kondo interaction.  $t_{ij}$  is the hopping integral, corresponding to a band dispersion  $\epsilon_{\mathbf{k}}$  whose density of states (DOS)  $\rho_0(\epsilon)$  is featureless.  $I_{ij}$  denotes the RKKY interaction; its

Fourier transform,  $I_{\mathbf{q}}$ , is the most negative at an antiferromagnetic (AF) wavevector  $\mathbf{Q}$  ( $I_{\mathbf{Q}} = -I$ ). The EDMFT approach leads to the effective impurity action

$$\begin{aligned} \mathcal{S}_{\text{imp}} &= \mathcal{S}_{\text{top}} + \int_0^\beta d\tau [h_{\text{loc}} S^z(\tau) + J_K \mathbf{S}(\tau) \cdot \mathbf{s}_c(\tau)] \\ &\quad - \int \int_0^\beta d\tau d\tau' \sum_\sigma c_\sigma^\dagger(\tau) G_{0,\sigma}^{-1}(\tau - \tau') c_\sigma(\tau') \\ &\quad - \frac{1}{2} \int \int_0^\beta d\tau d\tau' S^z(\tau) \chi_0^{-1}(\tau - \tau') S^z(\tau'). \end{aligned} \quad (2)$$

where  $\mathcal{S}_{\text{top}}$  is the Berry phase of the local moment, and  $h_{\text{loc}}$ ,  $G_{0,\sigma}^{-1}$ , and  $\chi_0^{-1}$  are the static and dynamical Weiss fields satisfying the self-consistency condition:

$$h_{\text{loc}} = -[I - \chi_0^{-1}(\omega = 0)] m_{\text{AF}}, \quad (3a)$$

$$\chi_{\text{loc}}(\omega) = \int_{-D}^I d\epsilon \rho_I(\epsilon) / [M(\omega) + \epsilon], \quad (3b)$$

$$G_{\text{loc},\sigma}(\omega) = \int_{-D}^I d\epsilon \rho_0(\epsilon) / [\omega + \mu - \epsilon - \Sigma_\sigma(\omega)]. \quad (3c)$$

Here,  $M(\omega)$  and  $\Sigma_\sigma(\omega)$  are respectively the spin and conduction-electron self-energies, which satisfy the Dyson(-like) equations:  $\Sigma_\sigma(\omega) = G_{0,\sigma}^{-1}(\omega) - G_{\text{loc},\sigma}^{-1}(\omega)$ , and  $M(\omega) = \chi_0^{-1}(\omega) + \chi_{\text{loc}}^{-1}(\omega)$ .  $m_{\text{AF}} = \langle S^z \rangle_{\text{imp}}$  is the staggered magnetization;  $\chi_{\text{loc}}(\omega)$  and  $G_{\text{loc},\sigma}(\omega)$  are the connected local spin susceptibility and local conduction electron Green's function, respectively. Finally,  $M(\omega)$  also specifies the lattice spin susceptibility:

$$\chi(\mathbf{q}, \omega) = 1/[I_{\mathbf{q}} + M(\omega)]. \quad (4)$$

As described in detail in Refs. [16, 17], the effective impurity action [Eq. (2)] can be rewritten in a Hamiltonian form, in which the dynamical Weiss fields are represented by a fermionic bath and a bosonic one. Through a canonical transformation, the fermionic coupling is reduced to a transverse field Ising model with an ohmic bosonic bath. Integrating out the two bosonic baths yields a form that is suitable for QMC studies:

$$\begin{aligned} \mathcal{S}'_{\text{imp}} &= \int_0^\beta d\tau [h_{\text{loc}} S^z(\tau) + \Gamma S^x(\tau) - \frac{1}{2} \int_0^\beta d\tau' S^z(\tau) \\ &\quad \times S^z(\tau') (\chi_0^{-1}(\tau - \tau') - \mathcal{K}_c(\tau - \tau'))]. \end{aligned} \quad (5)$$

Here,  $\mathcal{K}_c(i\omega_n) = \kappa_c |\omega_n|$  describes the ohmic dissipation;  $\kappa_c$  and  $\Gamma$  are determined by the longitudinal and transverse components of the Kondo coupling, respectively.

For the bNRG studies, we work in the real frequency domain by rewriting Eq. (5) in a Hamiltonian form:

$$\begin{aligned} \mathcal{H}'_{\text{imp}} &= h_{\text{loc}} S^z + \Gamma S^x \\ &\quad + \sum_p \tilde{g}_p S^z (\phi_p + \phi_{-p}^\dagger) + \sum_p \tilde{w}_p \phi_p^\dagger \phi_p, \end{aligned} \quad (6)$$

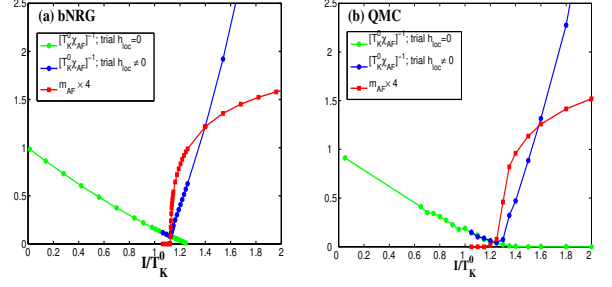


FIG. 1: (Color online) Inverse static AF susceptibility,  $\chi_{\text{AF}}^{-1} \equiv \chi(\mathbf{q} = \mathbf{Q}, \omega = 0)^{-1} = M(\omega = 0) - I$ , from the PM (trial  $h_{\text{loc}} = 0$ ; green circles) and AF (trial  $h_{\text{loc}} \neq 0$ ; blue circles) solutions and the AF order parameter  $m_{\text{AF}}$  (red squares), obtained from the bNRG (a) and QMC (b) methods. The lines are guides to eyes. See the main text for details.

where  $\tilde{\omega}_p$  and  $\tilde{g}_p$  are such that  $-\sum_p \frac{2\tilde{g}_p^2 \tilde{\omega}_p}{\omega^2 - \tilde{\omega}_p^2} = \tilde{\chi}_0^{-1}(\omega) \equiv \chi_0^{-1}(\omega) - \mathcal{K}_c(\omega)$ . The EDMFT procedure starts with a trial  $h_{\text{loc}}$  and  $\chi_0(\omega)$ . The bNRG iteration loop [21] is then used to solve the impurity model (6) for  $m_{\text{AF}}$  and  $\chi_{\text{loc}}(\omega)$  which, in turn, lead to updated  $h_{\text{loc}}$  and  $\chi_0^{-1}(\omega)$ . The procedure is repeated until convergence is achieved. For the most part, we consider two-dimensional magnetic fluctuations [17] as represented by a constant RKKY DOS  $\rho_I(\epsilon) \equiv \sum_{\mathbf{q}} \delta(\epsilon - I_{\mathbf{q}}) = (1/2I)\Theta(I - |\epsilon|)$ , with  $\Theta$  being the Heaviside function. In this case, Eq. (3b) yields

$$M(\omega) = I / \tanh[I\chi_{\text{loc}}(\omega)]. \quad (7)$$

We take the energy cutoff  $\omega_{\text{cutoff}} = 1$  and the parameters  $\Gamma = 0.75$  and  $\kappa_c = \pi$ , yielding  $T_K^0 \equiv 1/\chi_{\text{loc}}(\omega = 0, I = 0) \approx 0.71$ . In most cases (exceptions will be specified), we choose the NRG discretization parameter  $\Lambda = 2$ , keep  $N_b = 100$  bosonic states for the impurity site and 8 states for the other sites, and retain  $N_s = 60$  many-body states. To reach convergence, the difference between two consecutive iterations in  $h_{\text{loc}}$  as well as in  $\chi_0^{-1}(\omega)$  for each  $\omega$  is smaller than  $10^{-6}$ . Away from the transition region, 30 or so EDMFT iterations are sufficient. In the transition region, it takes as many as 2400 iterations. The large number of EDMFT iterations needed, together with the bNRG iterations for each EDMFT iteration, dictate the numerically intensive nature of our study.

The resulting phase diagram is summarized in Fig. 1(a). We observe a substantial drop of  $\chi_{\text{AF}}^{-1}$  from both sides, as well as of  $m_{\text{AF}}$ . Indeed, the magnetic order parameter  $m_{\text{AF}}$  vanishes continuously within the numerical uncertainty as  $I$  approaches the transition point  $I_{c1} (\approx 1.1228T_K^0)$ .

Fig. 2(a) shows  $\chi_{\text{loc}}(\omega)$  at various  $I$ , from around  $I = I_{c1}$  and beyond. Above a cutoff scale, the local susceptibility is logarithmically dependent on the frequency. Such a singular behavior signals the Kondo screening being critical, which is the hallmark of local quantum criticality. Fitting the slope of the logarithmic dependence in

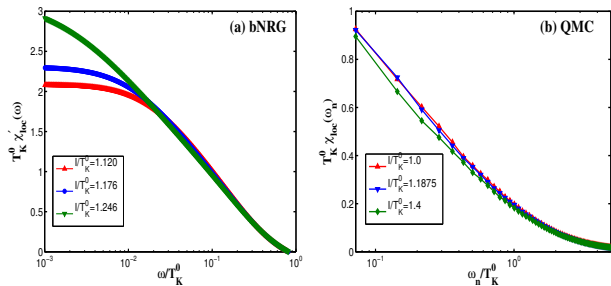


FIG. 2: (Color online) Frequency dependence of the local spin susceptibility at various values of  $I$  around the magnetic transition. (a)  $\chi'_{loc}(\omega)$  vs. the real frequency  $\omega$ , from bNRG; (b)  $\chi'_{loc}(\omega_n)$  vs. the Matsubara frequency  $\omega_n$ , from QMC.

terms of  $\alpha/2I$  yields an  $\alpha$  which is nearly constant (varying by less than 2%) in the shown range of  $I$ . Through the self-consistency Eq. (7) together with Eq. (4),  $\alpha$  is the critical exponent that appears in the dynamical AF spin susceptibility,  $\chi_{AF}(\omega) \equiv \chi(\mathbf{Q}, \omega)$ . Extrapolating to the bNRG continuum limit ( $\Lambda \rightarrow 1^+$ ) yields  $\alpha \approx 0.83$ . The low-frequency cut-off scale for the logarithmic dependence is relatively small, becoming of the order of  $\sim 10^{-2}T_K^0$  for the largest  $I$  we have reached as  $I$  is increased towards  $I_{c2}$  ( $\approx 1.26T_K^0$ ), the instability point of the paramagnetic solution signaled by a diverging  $\chi_{AF}$ ; this cut-off scale extrapolates to zero as  $I \rightarrow I_{c2}^-$ .

For comparison, the QMC results for the phase diagram and the Matsubara frequency dependence of the local dynamical spin susceptibility are shown in Figs. 1(b) and 2(b), respectively. At the gross level, the bNRG and QMC results are similar to each other.

At a fine level, the bNRG results contain some differences from their QMC counterparts. Major among these is the observation, as seen in Fig. 1(a), that  $I_{c2}$  is larger than  $I_{c1}$  by about 12%. In the QMC results, by contrast,  $I_{c2}$  equals  $I_{c1}$  within the numerical uncertainty of a few percents. To see whether this is unique to the bNRG results for the 2D magnetic fluctuations, we have carried out similar bNRG studies of the EDMFT phase diagram in the case of 3D magnetic fluctuations – as represented by a semicircular RKKY DOS,  $\rho_I(\epsilon) = \frac{2}{\pi T^2} \sqrt{T^2 - \epsilon^2} \theta(I - |\epsilon|)$ . The 3D case does not have the complication of a divergent local susceptibility, and a SDW solution is expected in the EDMFT approach [9, 16, 17]. We find that the magnetic transition is essentially continuous (with the upper bound of the order-parameter jump being 0.016), yet  $(I_{c2} - I_{c1})/I_{c1}$  is still non-zero (about 13%).

The observation of a continuous onset of the magnetic order parameter  $m_{AF}$  but, at the same time, different  $I_{c1}$  and  $I_{c2}$ , is unexpected. One possibility is that the dichotomy is inherent to the EDMFT equations. To address this, we return to the self-consistent equation for the magnetic order parameter, Eq. (3a). For a small  $h_{loc}$

(we have numerically determined that the magnetic solution is the same regardless of whether an infinitesimal finite value or a large value is chosen for the trial  $h_{loc}$ ), we have  $m_{AF} = -\chi_{loc} h_{loc} - a_3 h_{loc}^3 - a_5 h_{loc}^5 + \dots$ . Note, the linear coefficient is equal to  $-\chi_{loc}(\omega = 0)$  since, in Eq. (6),  $h_{loc}$  couples linearly to  $S^z$  only [28]. We can then rewrite Eq. (3a) as

$$r h_{loc} = -u h_{loc}^3 - v h_{loc}^5 + \dots, \quad (8)$$

where  $r = \chi_{loc}/\chi_{AF}$  is the quadratic coefficient of the corresponding static Landau function, and  $u = -a_3[\chi_{loc}^{-1} - \chi_{AF}^{-1}]$  and  $v = -a_5[\chi_{loc}^{-1} - \chi_{AF}^{-1}]$  are the quartic and sextic Landau coefficients. When  $u > 0$  (the alternative,  $u < 0$ , would lead to a large jump in  $m_{AF}$ , in contrast to what we have observed), we have a canonical case of a second-order transition at  $r = 0$  (in other words, a  $h_{loc} \neq 0$  solution cannot occur for any  $r > 0$ ). Through  $r = \chi_{loc}/\chi_{AF}$ , this implies that, at  $I_{c1}$  (the onset of the magnetic transition)  $\chi_{AF}$  diverges. This is the same condition for  $I_{c2}$ , where the paramagnetic solution goes away. So, within the EDMFT equations per se, a continuous onset in  $m_{AF}$  must coincide with a vanishing  $(I_{c2} - I_{c1})$ .

We are then led to search for numerical origins for the dichotomous observation, and have identified the primary source. Within bNRG, as in any NRG method, the imaginary part of the local susceptibility,  $\chi''_{loc}(\omega)$ , is calculated in terms of a set of Gaussian-broadened delta functions. The real part is in turn determined via the Kramers-Kronig relation, which we call  $\chi'_{loc, KK}(\omega)$ . The static local susceptibility can alternatively be calculated in terms of a) the differential response of the local magnetization *w.r.t.*  $h_{loc}$  or b)  $\sum_n | \langle n | S_z | 0 \rangle |^2 / (E_n - E_0)$ , where  $n$  labels all the many-body excited states and 0 the ground state. We find that the latter two methods yield essentially the same result, which we call  $\chi_{loc, static}$ . A key observation is that  $\chi_{loc, static}$  is larger than  $\chi'_{loc, KK}(\omega = 0)$  by a sizable amount (about 11.5% for  $\Lambda=2$ , in the 2D case). The quadratic Landau coefficient then becomes

$$r = \chi_{loc, static} / \chi_{AF} - [\chi_{loc, static} / \chi_{loc, KK}(\omega = 0) - 1]. \quad (9)$$

The onset of the magnetic transition (at  $r = 0$ ) then already occurs before  $\chi_{AF}$  diverges, which explains the observed  $I_{c1} < I_{c2}$ . In order to confirm our observation, we have implemented the simplest modification scheme to ensure that the Kramers-Kronig of the NRG-calculated  $\chi''_{loc}(\omega)$  yields a static local susceptibility that is equal to  $\chi_{loc, static}$ . We use, during each EDMFT iteration,  $\chi_{loc, static}$  for the  $\omega = 0$  component of  $\chi'_{loc}(\omega)$ , but retain  $\chi'_{loc, KK}(\omega)$  for all finite frequencies. The numerical effort is even larger, requiring more than 5000 EDMFT iterations near the transition. We find that  $I_{c1}$  is increased compared to that of the “vanilla” scheme. ( $I_{c2}$  is essentially unchanged, although the normalization parameter  $T_K^0$  is reduced.) Moreover, as shown in Fig. 3 for the 2D case,  $I_{c2} \approx I_{c1}$  [with a difference less than 1% (2%) in the

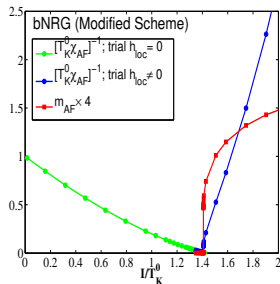


FIG. 3: (Color online) Inverse AF susceptibilities (PM, green circles; AF, blue circles) and the AF ordered moment (red squares), from the modified scheme, as described in the main text. The notations are the same as in Fig. 1.

2D (3D) case, with  $\Lambda = 2$ ].  $m_{AF}$  vs.  $(I - I_{c1})$  from the modified scheme is mostly comparable to that of Fig. 1(a) except for being steeper in the immediate vicinity of  $I_{c1}$  [when  $(I - I_{c1})/I_{c1}$  is within a few percents].

Since  $I_{c2}$  is where the AF susceptibility diverges, a coinciding  $I_{c1}$  and  $I_{c2}$  implies that the AF susceptibility diverges at the magnetic transition. This is clearly seen in the plots of the inverse AF susceptibility given in Fig. 3 [as well as at  $I_{c2}$  in Fig. 1(a)]. The magnetic transition is therefore second order within the numerical accuracy. For the 2D case, the divergent AF susceptibility automatically implies a divergent local susceptibility [as seen from Eqs. (3b,4), using a constant  $\rho_I$ ].

For  $I > I_{c2}$  [25], the nominally self-consistent paramagnetic solution has  $\max[2I\chi''_{loc}(\omega)] > \pi$ , which, through Eq. (7), yields an oscillatory  $M''(\omega)$  [26]. By contrast, in the Matsubara frequency domain, a nominally paramagnetic solution ( $h_{loc} = 0 = m_{AF}$ , but a finite Curie constant) exists for  $I > I_{c2}$ , which helped to determine the phase diagram [17]. It would be helpful to carry out QMC calculations at very low temperatures; the cluster-MC method [27], which may reach  $T \sim 10^{-5}T_K^0$ , is a promising route to pursue.

Independently, M. T. Glossop and K. Ingersent [29] have carried out NRG studies within the EDMFT approach to the same Kondo lattice model. They used the NRG method of Ref. [22], in which the Kondo coupling to the conduction electrons are directly treated. (By contrast, we have mapped the Kondo coupling to an ohmic dissipative bath and applied the bNRG method of Ref. [21].) In Ref. ([29]b), they adopted a somewhat different modification scheme to ensure the consistency between the static local susceptibilities from two ways of calculation within NRG. In spite of these differences in methods, the results from the two studies are largely compatible with each other.

To summarize, we have carried out bosonic numerical renormalization group studies of the extended dynamical mean field theory of a Kondo lattice model. The local spin susceptibility has a logarithmic frequency de-

pendence – signifying the critical Kondo screening – and the magnetic transition is consistent with being second order. These results provide evidence for local quantum criticality and hence are important for experiments in heavy fermions and quantum phase transitions in general. Finally, our study has also advanced the understanding of the numerical renormalization group, a venerable method [30] in the area of correlated systems.

**Acknowledgments:** We thank M. T. Glossop, K. Ingersent, G. Kotliar, Z. Nussinov, G. Ortiz, P. Sun, N.-H. Tong, and L. Zhu for useful discussions. We dedicate this work to the memory of the late Daniel R. Grempel, with whom two of us (JXZ and QS) had collaborated on QMC studies. We acknowledge the support of the U.S. DOE at LANL under Contract No. DE-AC52-06NA25396 and Grant Nos. LDRD-DR X9GT and WSR JA2W/JHU1 (JXZ), NSF Grant No. DMR-0424125 and the Robert A. Welch Foundation (SK and QS), and the DFG collaborative research center SFB 484 (RB).

- 
- [1] H. v. Löhneysen *et al.*, cond-mat/0606317.
  - [2] J. A. Hertz, Phys. Rev. B **14**, 1165 (1976).
  - [3] T. Moriya, *Spin Fluctuations in Itinerant Electron Magnetism* (Springer, Berlin, 1985).
  - [4] A. J. Millis, Phys. Rev. B **48**, 7183 (1993).
  - [5] A. Schröder *et al.*, Nature **407**, 351 (2000).
  - [6] M. Aronson *et al.*, Phys. Rev. Lett. **75**, 725 (1995).
  - [7] S. Paschen *et al.*, Nature **432**, 881 (2004).
  - [8] R. KÜchler *et al.*, Phys. Rev. Lett. **91**, 066405 (2003)
  - [9] Q. Si *et al.*, Nature **413**, 804 (2001); Phys. Rev. B **68**, 115103 (2003).
  - [10] P. Coleman *et al.*, J. Phys.: Condens. Matter **13**, R723 (2001). C. Pépin, Phys. Rev. Lett. **94**, 066402 (2005); J. Rech *et al.*, *ibid.* **96**, 016601 (2006).
  - [11] T. Senthil, M. Vojta, and S. Sachdev, Phys. Rev. B **69**, 035111 (2004).
  - [12] Q. Si and J. L. Smith, Phys. Rev. Lett. **77**, 3391 (1996); J. L. Smith and Q. Si, Phys. Rev. B **61**, 5184 (2000).
  - [13] R. Chitra and G. Kotliar, Phys. Rev. Lett. **84**, 3678 (2000); H. Kajueter, Ph.D. thesis Rutgers Univ. (1996).
  - [14] S. Doniach, Physica B **91**, 231 (1977).
  - [15] C. M. Varma, Rev. Mod. Phys. **48**, 219 (1976).
  - [16] D. R. Grempel and Q. Si, Phys. Rev. Lett. **91**, 026401 (2003).
  - [17] J.-X. Zhu *et al.*, Phys. Rev. Lett. **91**, 156404 (2003).
  - [18] P. Sun and G. Kotliar, Phys. Rev. Lett. **91**, 037209 (2003).
  - [19] P. Sun and G. Kotliar, Phys. Rev. B **71**, 245104 (2005).
  - [20] Q. Si, J.-X. Zhu, and D. R. Grempel, J. Phys.: Condens. Matter **17**, R1025 (2005).
  - [21] R. Bulla *et al.*, Phys. Rev. Lett. **91**, 170601 (2003); Phys. Rev. B **71**, 045122 (2005).
  - [22] M. T. Glossop and K. Ingersent, Phys. Rev. Lett. **95**, 067202 (2005); Phys. Rev. B **75**, 104410 (2007).
  - [23] A. Kuklov *et al.*, Phys. Rev. Lett. **93**, 230402 (2004); A. W. Sandvik and R. G. Melko, cond-mat/0604451.
  - [24] T. Senthil *et al.*, Science **303**, 1490 (2004).
  - [25] The  $I$  beyond which nonanalyticity develops differs from

the extrapolated  $I_{c2}$  by about 0.5% (for  $\Lambda = 2$ ), which we attribute to numerical uncertainty.

- [26] S. Burdin *et al.*, Phys. Rev. B **67**, 121104(R) (2003); K. Haule *et al.*, *ibid.* **68**, 155119 (2003).
- [27] F. Niedermayer, Phys. Rev. Lett **61**, 2026 (1988).
- [28] This is equivalent to saying [20] that the effective RKKY interaction generated by the conduction electrons is excluded on the ordered side, as it inherently is on the paramagnetic side. Otherwise, a particle-hole bubble would

contribute an additional term to the quadratic Landau coefficient on the ordered side [the parameter  $r$  in Eq. (8)] [19], leading to a strongly first order transition: indeed,  $(I_{c2} - I_{c1})/I_{c1}$  is larger than 100% in Ref. [18].

- [29] (a) M. T. Glossop and K. Ingersent, cond-mat/0607566v1; (b) *ibid.*, cond-mat/0607566v2.
- [30] R. Bulla, T. Costi and T. Pruschke, cond-mat/0701105.